Springer

KSME

Journal of Mechanical Science and Technology 24 (3) (2010) 711~719
www.springerlink.com/content/1738-494x
DOI 10.1007/s12206-010-0121-1

Creep-fatigue design studies for a sodium-cooled fast reactor with tube sheet-to-shell structure subjected to elevated temperature service†

Gyeong-Hoi Koo and Jae-Han Lee
Korea Atomic Energy Research Institute

(Manuscript Received October 15, 2009; Revised January 11, 2010; January 26, 2010)

Abstract

In this paper, creep-fatigue damage under elevated temperatures is investigated for a tube sheet-to-shell structure, which is one of the main structures under Gen-IV class 1 components. To do this, detailed step-by-step procedures, including the elastic structural analysis and the ASME-NH code application, are described for a defined representative load cycle. From the sensitivity studies for various design parameters, such as hold time duration, shell thickness, and operating temperature, it is found that a reduction of thickness can decrease the thermal bending stresses, but the negative effect is that it may increase the primary stress and enhance the creep damage. The normal operating temperature is the most significant parameter in the creep-fatigue design.

Keywords: Creep-fatigue; Sodium-cooled fast reactor; ASME-NH; Elevated temperature design; Creep damage; Gen-IV

1. Introduction

Recently, the elevated temperature component design for Generation IV (Gen-IV) reactors has become an interesting topic worldwide. To develop industry codes and standards applicable to the elevated temperature design, international efforts are exerted on the ASME Boiler and Pressure Vessel Code, Section III, Division 1-Subsection NH (ASME-NH) [1], RCC-MR [2], and DDS [3].

Studies have been performed to establish practical procedures for an elevated temperature structural design through industry codes and standards, such as the ASME-NH and RCC-MR [4, 5]. In these studies, the step by step calculations of the structural integrity items, including the primary stress limits, inelastic strain limits, and creep-fatigue limits, and the hand-calculated results are described in detail. Even the evaluation procedures are very clear and straightforward. However, hand calculations involve a long evaluation time due to the complexity of design rules. Therefore, it is not easy to develop the structural design concept through the design-by-analysis rule and consideration of the various design parameters.

To resolve the problems in the practical application of the ASME-NH rules for class 1 components in elevated temperature service, the SIE ASME-NH computer code, which includes the design material database, has been developed using the analysis rule to implement the whole design-by-analysis rule, [6]. This computer code makes the structural integrity evaluation for elevated temperature structures fast and accurate, with the least amount of errors. The user's manual for this computer code [7] is highly helpful in understanding the main application procedures.

In this paper, creep-fatigue design studies are investigated for the tube sheet-to-cylindrical shell structure, which is one of the main structures under the Class 1 components of a sodium-cooled fast reactor, by using the SIE ASME-NH code. Before using the SIE ASME-NH input data, the results of the thermal transient analysis and the elastic stress analysis are also described in detail. Based on the specified original design parameters, design case studies using the ASME-NH code rules are performed to determine the creep-fatigue limits for a specified representative design load. This study is expected to provide practical design procedures through the analysis of class 1 components subjected to an elevated temperature service.

2. Design descriptions

2.1 Descriptions of design features

The tube sheet-to-cylindrical shell structure, which is designed to be used under elevated temperature service, is one of the important shapes of main components in GEN-IV reactors, such as the intermediate heat exchanger (IHX), steam generator, and reactor internals. These are all classified as Class 1

† This paper was recommended for publication in revised form by Associate Editor Jooho Choi

*Corresponding author. Tel.: +82 42 868 2950, Fax.: +82 42 861 7697
E-mail address: ghkoo@kaeri.re.kr

Table 1. Design material properties.

Temp. (℃)	316 SS					
	Conductivity (J/s-m-℃)	Expansion (m/m-℃) $\times 10^{-6}$	Specific Heat (J/kg-℃)	Young's Modulus (GPa)	Density (kg/m^3)	Poisson's ratio
21	14.1	15.1	465.6	195.0	8000.0	0.3
100	15.4	16.4	486.0	189.0	7932.0	0.3
200	16.8	17.0	508.0	183.0	7889.0	0.3
300	18.3	17.5	529.0	176.0	7846.0	0.3
400	19.7	17.9	550.0	169.0	7803.0	0.3
500	21.2	18.3	571.0	160.0	7760.0	0.3
600	22.6	18.7	592.0	151.0	7717.0	0.3

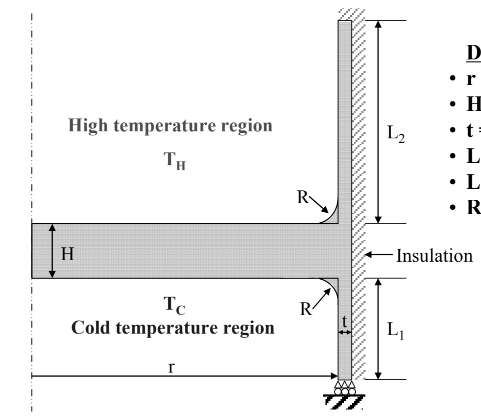

Fig. 1. Geometrical shape and dimensions.

components in a nuclear power plant design. The target design lifetime and the normal operating temperature are 60 years and 550°C respectively. The selected structural material is a 316 stainless steel. The temperature-dependent physical material properties used in the analysis are listed in Table 1.

Fig. 1 shows the axisymmetric geometrical shape and dimensions to be used in the structural integrity evaluation. The thicknesses of the tube sheet and the cylindrical shell are 50 and 10 cm respectively. The inner diameter of the cylinder shell is 3 m, and the lengths of the cylindrical shell joined to the tube sheet are extended enough to neglect the end effects. The fillet radii at junction parts are all tentatively designed to be 0.2 m.

The pool region above the tube sheet is assumed to be filled with hot coolant and the lower pool is filled with cold coolant. The outer surface of the cylindrical shell is designed to be thermally insulated.

2.2 Design load conditions

For the structural integrity evaluation, the design load conditions are assumed to represent one of the several thermal transients and internal pressure loads. In this paper, the operating conditions where the operation changes from a hot standby condition (300°C) to a full power condition (550°C) and vice versa are considered. There is a total 1,000 load cycles, each resulting from an operating time of 500 hours per one cycle when the total elevated temperature service time is defined to be 500,000 hours (about 95% of 60 years).

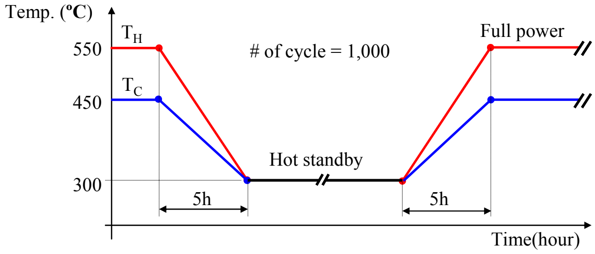

Fig. 2. Representative thermal load cycle type.

Fig. 2 presents the thermal cycle for hot pool and cold pool temperature transients. The hot and cold pool temperatures are 550 and 450°C, respectively, for a steady state full power operation. Both temperatures linearly decrease to the hot standby temperature of 300°C for 5 hours during a cool-down operation. The heating operation is defined as the reversed process of a cool-down operation with the same duration for the temperature. In the actual setup, the duration of heating and cooling is defined very conservatively based on the structural integrity. This is conventionally used in pressurized water reactor (PWR) design specifications.

For the primary load, the maximum internal pressure on the whole inner surface is conservatively considered to be 10 atm (≈1.0 MPa). In general, the sodium-cooled fast reactor is operated in atmospheric pressure. Then, the design pressure is defined to be less than 5 atm. The dead weight and the dynamic load, including the seismic load, which can invoke a short-term creep effect, are not considered in this study.

2.3 Design code and standards

The design code and standards used in elevated temperature structural integrity evaluation is the ASME-NH for Class 1 components under elevated temperature service [1]. This code provides the design-by-analysis rules to prevent structural failures from time-dependent damages, such as creep rupture, excessive creep deformation, cyclic creep ratcheting, creep-fatigue, creep crack growth, and creep buckling.

To enhance the accuracy of the evaluation results and reduce the engineering costs, the SIE ASME-NH computer program [7] implementing the ASME-NH rules is used in this paper. The step-by-step procedures of the creep-fatigue evaluations by the SIE ASME-NH program are as follows:

Fatigue damage evaluations

Step 1: Define the complete load cycle types

Step 2: Perform the elastic strain analysis for each cycle type, j

Step 3: Calculate the elastic strain time history for each cycle type, j

Step 4: Select one of the extreme time points for the cycle (set subscript o)

Step 5: Calculate strain ranges for all the components at each time point:

$\Delta\varepsilon_{xi} = \varepsilon_{xi} - \varepsilon_{xo}$, $\Delta\varepsilon_{yi} = \varepsilon_{yi} - \varepsilon_{yo}$

Step 6: Calculate the equivalent strain range for each point in time as:

$$\Delta\varepsilon_{equi,i} = \frac{\sqrt{2}}{2(1+\nu^*)}\Big[\left(\Delta\varepsilon_{xi} - \Delta\varepsilon_{yi}\right)^2 + \left(\Delta\varepsilon_{xi} - \Delta\varepsilon_{yi}\right)^2 + \left(\Delta\varepsilon_{xi} - \Delta\varepsilon_{yi}\right)^2 + \frac{3}{2}\left(\Delta\gamma_{xyi}^2 + \Delta\gamma_{yzi}^2 + \Delta\gamma_{zxi}^2\right)\Big]^{1/2}$$

Step 7: Define $\Delta\varepsilon_{max} = Max\ (\Delta\varepsilon_{xiequiv,i})$

Step 8: Modify $\Delta\varepsilon_{max}$ with a local geometric stress concentration and the multiaxial effects

Step 9: Calculate the total strain range as $\varepsilon_t = K_v\Delta\varepsilon_{\mathrm{mod}} + K\Delta\varepsilon_c$

Step 10: Find the allowable number of cycles, N_d, from the design fatigue curves corresponding to ε_t

Step 11: Calculate the fatigue damage by $\sum_j^p \left(\frac{n}{N_d}\right)_j$

Creep damage evaluations

Step 1: Define the total number of hours expended at an elevated temperature, $t_{H.}$

Step 2: Define the hold temperature, T_{HT}

Step 3: Define the average cycle time: $\overline{t_j} = t_H / n_j$

Step 4: Determine the stress level, $S_j|\varepsilon_t$, from time independent isochronous stress-strain curve corresponding to $T_{HT.}$

Step 5: Obtain the stress relaxation time history curve at dwell stress, S_j, and a hold temperature, $T_{HT.}$

Step 6: Modify the stress relaxation time history curve by considering the load-controlled transient effect.

Step 7: Define the cycle transient temperature.

Step 8: Repeat Steps 3-7 to make j=1 for the P sets of the stress relaxation time histories and superimpose these onto the results in the enveloped stress-time history.

Step 9: Determine the integration time step size, $(\Delta t)_k$, the stress, $(S)_k/K'$, and the temperature, $(T)_k$.

Step 10: Obtain the allowable time duration, $(T_d)_k$, for each time interval from the expected minimum stress-to-rupture curve.

3. Thermal and elastic stress analyses

To obtain the elastic analysis results for the specified loads, finite element analyses are performed with the ANSYS computer program [8]. Fig. 3 shows the axisymmetric finite element analysis model with a 2-D thermal solid element, designated as PLANE55, for thermal transient analysis and a 2-D structural solid element, designated as PLANE42, for stress analysis. This model is prepared through the after adequate checking because the element mesh size and shape can significantly affect the analysis results, especially in the region of discontinuity, i.e., fillet junction parts in the figure.

A detailed thermal transient analysis is carried out to determine the metal temperature data and to calculate the thermal stress. For the maximum primary stress calculations, the stress analysis is carried out for an internal pressure load.

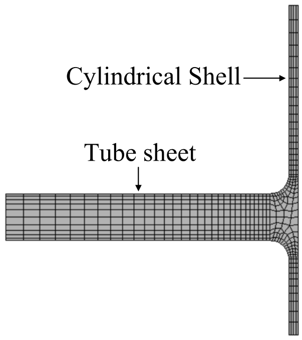

Fig. 3. Axisymmetric finite element analysis model.

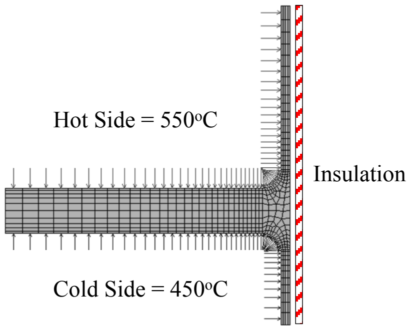

Fig. 4. Applied thermal boundary conditions.

3.1 Thermal transient analysis

The thermal boundary conditions used for a steady state full power operation are shown in Fig. 4. The general assumptions for a thermal transient analysis are as follows:

- The outer surface is assumed to be thermally insulated.
- The heat flux through the shell end thickness is neglected during analysis.
- The coolant in the hot pool region is flowing rapidly, therefore, the film coefficient is assumed to be very large.
- The coolant in the cold pool region is flowing much slower than the hot coolant. Then, it is assumed that the film coefficient is 600 J/°C-sec-m^2.

The calculated temperature distributions are presented in Figs. 5(a) and (b) by a half axisymmetric expansion for a steady state full power operation and for the end of the cool-down operation at t=5 h. As shown in the figures, the location of the maximum temperature at the end of the cool-down operation is the junction part of the outer surface of shell. Therefore, it is expected that the maximum thermal stress occurs in this location after the cool-down operation.

3.2 Thermal stress analysis and results

The thermal stress-time history responses are calculated from the results of the previous thermal transient analysis. In this calculation, the tube sheet is considered as a solid plate without perforated holes for the pre-conceptual design investigation. Figure 6 shows the thermal stress distributions during

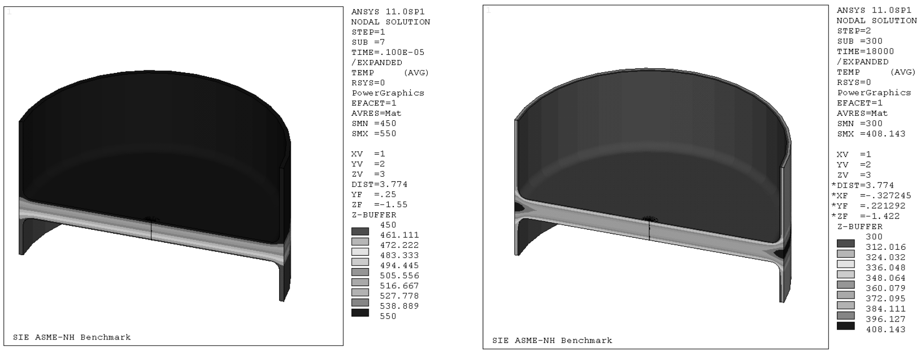

(a) At steady state full power operation (b) At end of cool-down (t = 5 hours)

Fig. 5. Results of temperature distributions during cool-down operation.

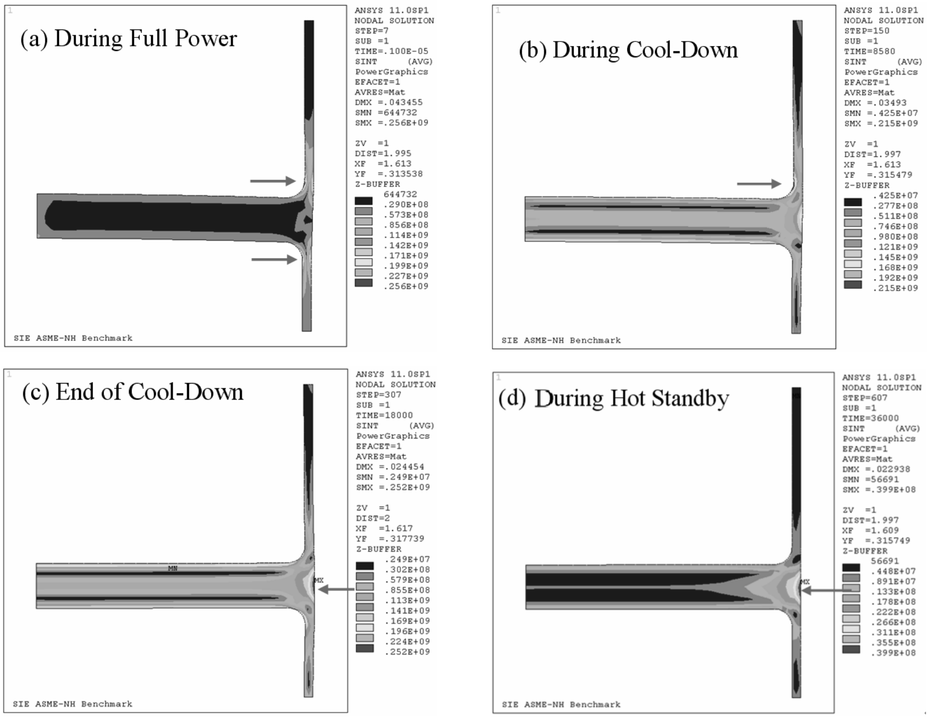

Fig. 6. Thermal stress distributions during the cool-down operation.

the cool-down and hot standby operations. The maximum stress points continuously move throughout the structure. During the steady state full power operation, the maximum thermal stress (256 MPa) occurs at the fillet regions. While operating the cool-down process, the maximum stress occurs only at the upper fillet region, but it moves to the junction part of the outer surface of the shell just after the cool-down operation. Fig. 7 shows the heating condition. During the steady state hot standby condition, the maximum stress (219 MPa) occurs at the upper fillet part. While operating the heating process, the maximum stress moves to the lower fillet part.

The stress analysis results, together with the primary stress results, are used to determine the critical section of creep-fatigue damage.

3.3 Primary stress analysis and results

An internal pressure load (1.0 MPa) is applied to the inside surface of both the upper and lower pool regions. Figure 8 reveals the primary stress distributions and deflection shape based on the half axisymmetric expansion model. As shown in the figure, the maximum primary stress is about 33 MPa, occurring at both the upper and lower junction parts between the tube sheet and the cylindrical shell. The stress components of the upper junction part are classified into sections and investigated. Fig. 9 presents the linearized membrane stress, membrane plus bending stress, and total stress intensities. The stress intensity pertains to the difference between the algebraically largest principal stress and the algebraically smallest

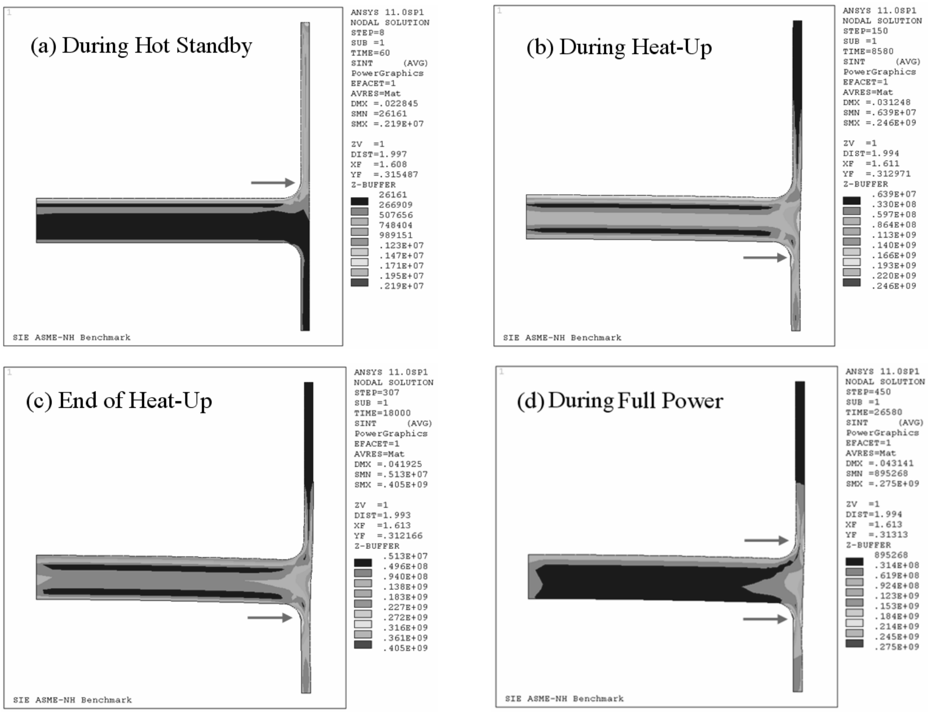

Fig. 7. Thermal stress distributions during the heating operation.

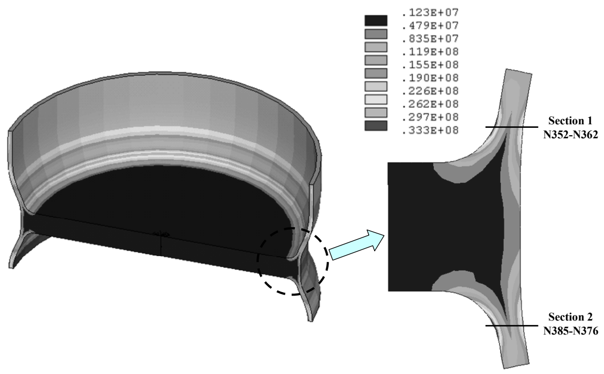

Fig. 8. Primary stress intensity distributions.

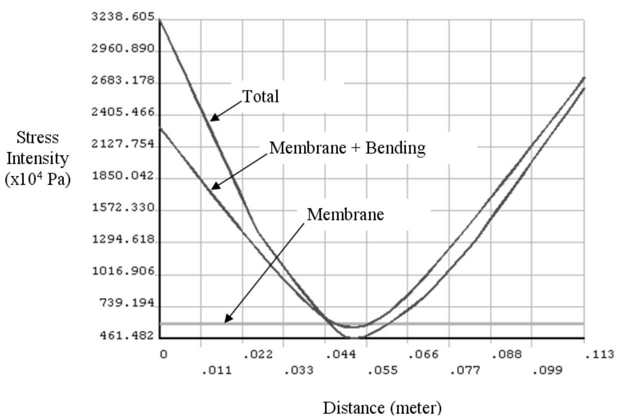

Fig. 9. Linearized stress intensities for primary load.

principal stress at a given point. The total stress intensity is larger in the inner surface than on the outer surface, but the bending stress is larger on the outer surface than in the inner surface. Due to a larger peak stress, fatigue damage can be larger in the inner surface than on the outer surface. Due to a larger bending stress, the creep damage can be larger on the outer surface than in the inner surface .

4. Structural integrity evaluations

4.1 Determination of evaluation sections

Based on the thermal stress and primary stress analysis results, the maximum stresses occur at both the upper and lower junction parts between the tube sheet and the cylindrical shell. The metal temperature affects creep damage calculation much more than any other parameter. Therefore, even though high stresses occur at the lower junction part in Fig. 9, the creep damage may not be as significant in there because the maximum wall averaged temperature is low at the cold pool region during normal operations. However, use of a hot pool coolant can induce significant creep damages at the upper junction part. Therefore, the section of the upper junction part in Fig. 9 is selected for the creep-fatigue evaluation.

4.2 Generation of input data for SIE ASME-NH

To evaluate the structural integrity for the calculated results from the elastic analysis, it is necessary to calculate the linearized stresses for the selected evaluation section and the

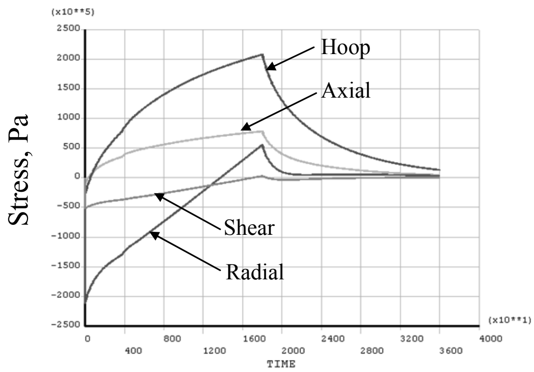

(a) For the cool-down operation

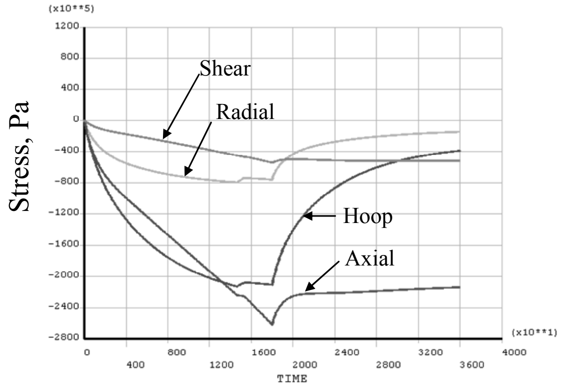

(b) For the heating operation

Fig. 10. Thermal stress-time responses.

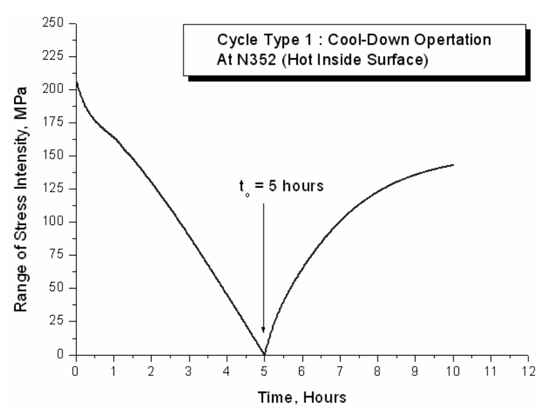

(a) For cool-down operation

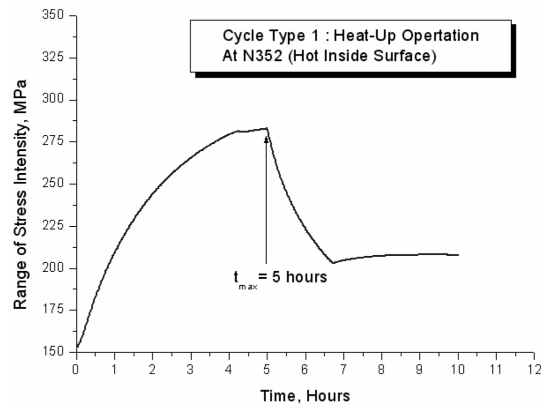

(b) For heat-up operation

Fig. 11. Range of thermal stress intensity time history responses.

total strain components for the inner and outer nodal points at two time points, which results in the maximum secondary stress and strain range.

Fig. 10 presents the secondary stress component-time history for an inner surface node in an evaluation section. As shown in Fig. 10(a) of the cool-down operation, the maximum stress component is a radial stress at the steady state full power operation (t=0 s). Just after the end of the cool-down operation, the tensional hoop stress becomes the maximum stress component (t=18,000 s). For the heating operation, the compressive axial stress is the maximum stress component just after the heat-up operation (t=18,000 s).

To determine the time points resulting in the maximum stress intensity range, the stress intensity-time curve is plotted (Fig. 11) both for the cool-down and heating operations. The time points in the maximum stress intensity is at t=5.0 hours (18,000 s) both for the cool-down and heating operations.

The linearized stresses at the determined time points are graphed in Fig. 12. For the cool-down operation in Fig. 12(a), a maximum bending stress intensity occurs at the inner surface. For the heating operation in Fig. 12(b), a significant bending stress occurs on the outer surface. The elastic strain components are also obtained at determined time points to calculate the maximum equivalent strain range for fatigue damage evaluation.

The input temperature data required for an elevated temperature structural integrity evaluation are as follows:

- Maximum and minimum wall-averaged temperature: [550°C, 300°C]
- Hot and cold temperatures during the cycle: [550°C, 300°C]
- Wall-averaged metal temperature for the stress extremes: [550°C, 300°C], Inner; [517°C, 332°C], Outer
- Maximum metal temperature during the cycle: [550°C: inner; 517°C: outer]
- Hold Temperature: [540°C]

The design lifetime for evaluation is 500,000 hours, and the total number of cycles is 1,000. A 0.1 hour time interval is used for the calculation of the creep damage from the established stress relaxation-time curve.

4.3 Results and discussions

4.3.1 Primary load limits

The cycle type used in this paper is a normal service level (A). The evaluation results for the primary load limit criteria

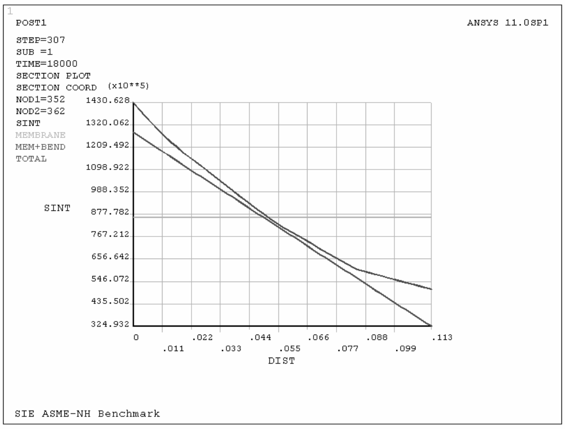

(a) For cool-down operation

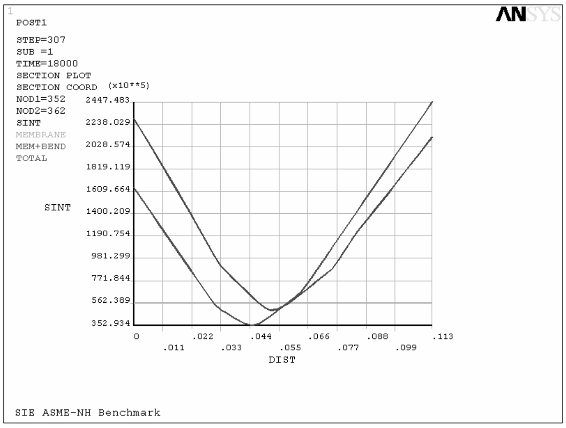

(b) For heat-up operation

Fig. 12. Linearized stress intensities for thermal load.

are as follows:

Inner Surface:
- Membrane Stress : P_m = 5.9 MPa < S_{mt} = 73.0 MPa (Satisfied)
- Membrane + bending stress : $P_L + P_b$ = 23.0 MPa < KS_m = 158.0 MPa (Satisfied)
- Membrane + bending stress : $P_L + P_b/K_t$ = 18.3 MPa < S_t = 73.0 MPa (Satisfied)
- Use-fraction-sum (P_m) : t_i/t_{im} = 0.343 < 1.0 (Satisfied)
- Use-fraction-sum ($P_L + P_b/K_t$) : t_i/t_{ib} = 0.390 < 1.0 (Satisfied)

Outer Surface:
- Membrane Stress : P_m = 5.9 MPa < S_{mt} = 73.0 MPa (Satisfied)
- Membrane + bending stress : $P_L + P_b$ = 27.3 MPa < KS_m = 158.0 MPa (Satisfied)
- Membrane + bending stress : $P_L + P_b/K_t$ = 22.5 MPa < S_t = 73.0 MPa (Satisfied)
- Use-fraction-sum (P_m) : t_i/t_{im} = 0.343 < 1.0 (Satisfied)
- Use-fraction-sum ($P_L + P_b/K_t$) : t_i/t_{ib} = 0.409 < 1.0 (Satisfied)

The primary load limits for a given internal pressure load satisfy the ASME-NH rules with enough margins. In contrast to the conventional PWR design, the sodium-cooled reactor is operating almost in an atmospheric pressure. The primary internal pressure load does not govern the structural design margins.

4.3.2 Strain and creep-fatigue limits

For the deformation and the inelastic strain limit evaluation, the design satisfaction can be confirmed by using the elastic analysis method in the ASME-NH T-1320 rules. The evaluation results are as follows:

Inner Surface:

Primary stress index : $X = \left(P_L + \dfrac{P_b}{K_t}\right)_{\max} \div S_y$
$= 18.3 \text{ MPa} \div 124 \text{ MPa}$
$= 0.148$

Secondary stress index: $Y = (Q_R)_{\max} \div S_y$
$= 185.8 \text{ MPa} \div 124 \text{ MPa}$
$= 1.498$

Test No. A-1: (X + Y) = 1.646 > S_a/S_y = 1.0 (Not satisfied)

Outer Surface:

Primary stress index: $X = \left(P_L + \dfrac{P_b}{K_t}\right)_{\max} \div S_y$
$= 22.5 \text{ MPa} \div 124 \text{ MPa}$
$= 0.181$

Secondary stress index: $Y = (Q_R)_{\max} \div S_y$
$= 264.1 \text{ MPa} \div 124 \text{ MPa}$
$= 2.130$

Test No. A-1: (X + Y) = 2.311 > S_a/S_y = 1.0 (Not satisfied)

Due to an excessive secondary stress range, the elastic analysis method cannot be used to derive the inelastic strain limits.

As an alternative, the effective creep ratchet stresses are calculated to follow the simplified inelastic analysis method provided in the ASME-NH T-1330 rules. The calculated effective creep stresses, σ_c, are 111.3 and 203.1 MPa for the inner and outer surfaces, respectively. From these results the total creep ratcheting strain is calculated as 3.82% for the inner surface. This greatly exceeds the limit value (1.0%) for the base metal. For the outer surface, the effective creep stress exceeds the yield strength at the hot end as σ_c = 203.1 MPa > S_{yH} = 117.3 MPa. Therefore, with compliance to the ASME-NH, this rule is not applicable for the thermal cycle type used in this paper. The alternative rule of Test No. B-3, which is applicable for cycle types in the regimes of the ratchet, is also not applicable because the evaluation section in this paper is within local structural discontinuity alone.

The calculated fatigue and creep damages for the inner surface are 0.137 and 3.33, respectively. This result greatly exceeds the creep-fatigue envelop limit. For the outer surface, the effective creep ratchet stress level, $1.25\sigma_c$=253.9 MPa, exceeds the values designed for the material, as provided by the ASME-NH code.

In conclusion, it is necessary to improve or modify the design conditions in order to meet the ASME-NH design rules. To do this, sensitivity studies are carried out to improve the design parameters, including the elevated temperature service lifetime (total hold time), shell thickness (to reduce the maximum thermal bending stress), and normal operating temperature.

5. Case studies for design improvements

5.1 Definition for design cases

To improve the design parameters specified in the previous design problem, three design cases are considered as follows:

- Design Case 1: HT = 300,000 hours, TH = 10 cm, OT = 550°C
- Design Case 2: HT = 300,000 hours, TH = 5 cm, OT = 550°C
- Design Case 3: HT = 300,000 hours, TH = 10 cm, OT = 510°C

In the above parameters, HT, TH, and OT indicate the total hold time, shell thickness, and normal operating temperature, respectively. For all these cases, the total hold time of the elevated temperature during a whole design lifetime is reduced to 300,000 hours. Therefore, the Design Case 1 is the same as the original design, except for the hold time. The Design Case 2 is considered to investigate the effect of shell thickness on the basis that a reduced shell thickness may result in a maximum thermal bending stress. In the Design Case 3, the normal operating temperature is reduced to 510°C.

5.2 Evaluation of the results and discussions

The thermal and structural analyses and the evaluation processes in Sections 3 and 4 are repeated step-by-step with the SIE ASME-NH computer code for all design modification cases. Table 2 presents the summary of the analysis and the evaluation results for primary limits. As shown in the table, the primary stress intensities increase in Design Case 2 due to the reduced shell thickness. Specifically, the bending stress intensity in the Design Case 2 increases about two-fold compared to that of Design Cases 1 and 3. The total use-fraction-sum is reduced in all design cases due to the reduced total hold time, but it is significantly reduced in Design Case 3, especially due to the lower operating temperature. This means that the normal operating temperature, in combination with the hold time duration, is a highly sensitive parameter in that determines the creep damage.

Table 3 presents the summary results of the creep-fatigue damage evaluations, including various related calculation values. The main key conclusions from the evaluation results are as follows:

Table 2. Primary load evaluations for the design cases.

Case No.	Section	P_m, MPa	P_L+P_b, MPa	P_L+P_b/K_t, MPa	UFS (t/t_m)	UFS (t/t_b)
1	Inside	5.9	23.0	18.3	0.206	0.234
	Outside	5.9	27.3	22.5	0.206	0.246
2	Inside	8.8	47.7	37.8	0.212	0.299
	Outside	8.8	56.3	46.0	0.212	0.339
3	Inside	5.9	23.0	18.3	0.092	0.103
	Outside	5.9	27.3	22.5	0.092	0.106

Table 3. Creep-fatigue damage evaluations for the design cases.

Case No.	Location in Section	$1.25\,\sigma_c$, MPa	$\Delta\varepsilon_{ep}$,%	$\Delta\varepsilon_c$,%	$\Delta\varepsilon_t$,%	S_j, MPa	T_{HT},℃	Fatigue damage	Creep damage
1	Inside	139.1	0.2391	0.0044	0.2435	140.6	540	0.1304	2.051
	Outside	253.9	0.1578	-	-	-	-	-	-
2	Inside	242.2	0.1472	-	-	-	-	-	-
	Outside	309.7	-	-	-	-	-	-	-
3	Inside	99.6	0.2421	0.0001	0.2422	0.2422	142.0	0.068	0.527
	Outside	168.2	0.1105	0.0012	0.1117	0.1117	124.5	0.864E-3	0.775

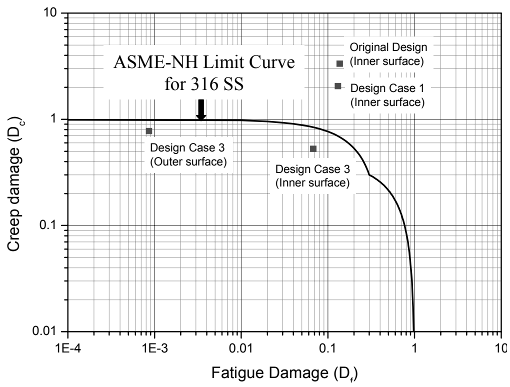

Fig. 13. Results of creep-fatigue damage evaluations.

- The modified Design Case 1, which reduces the total design lifetime to 300,000 hours, instead of 500,000 hours, results in a lower creep strain increment but still can not satisfy the ASME-NH rules.
- The modified Design Case 2, which reduces the total design lifetime to 300,000 hours and the thickness of the side cylinder to 5 cm (from 10 cm), with the purpose of mitigating the thermal bending stress, results in smaller thermal bending stresses but larger primary stresses due to internal pressure. Therefore, this case has no design advantage in creep-fatigue damage mitigation.
- The modified Design Case 3, which reduces the normal operating temperature to 510°C, satisfies the creep-fatigue damage limit of the ASME-NH rules using a certain margin.
- In conclusion, it is revealed that the maximum operating temperature is the most critical parameter affecting the creep-fatigue design.

The results of the creep-fatigue damage evaluations for all design cases are plotted on the creep-fatigue interaction curve (Fig. 13) as the ASME-NH criteria for a 316 stainless steel.

6. Conclusions

In this paper, the creep-fatigue design for a tube sheet-to-shell structure, which is one of the main structural parts for Gen-IV Class 1 components subjected to elevated temperature service, is investigated for a specified representative operating cycle type. From the various design case studies considering hold time duration, shell thickness, and normal operating temperature, it is found that the reduction of the thickness can decrease the thermal bending stresses but may cause negative effects by increasing the primary stress and enhancing the creep damage. The level of the normal operating temperature is revealed as the most significant design parameter in the creep-fatigue design. Therefore, since the core outlet temperature can significantly affect the elevated temperature component, the designer should determine the proper design temperature in terms of the economic benefits of the structural component design, plant performance, and core design.

Acknowledgments

This project has been carried out under the Nuclear R & D Program by MEST.

References

[1] ASME Boiler and Pressure Vessel Code, Section III, Subsection NH, (2007).
[2] RCC-MR, Design and Construction Rules for Mechanical Components of FBR Nuclear Islands, AFCEN (2002).
[3] Elevated Temperature Structural Design Guide for Class 1 Components of Prototype Fast Breeder Reactor, PNC N241-84-08, PNC, (1984).
[4] G. H. Koo and B. Yoo, Elevated Temperature Design of KALIMER Reactor Internals Accounting for Creep and Stress Rupture Effects, *Journal of the Korean Nuclear Society*, 32 (6) (2000) 566-594.
[5] G. H. Koo and B. Yoo, Evaluation of Creep-Fatigue damage of KALIMER Reactor Internals Using the Elastic Analysis Method in RCC-MR, *Journal of the Korean Nuclear Society*, 33 (6) (2001) 566-584.
[6] G. H. Koo and J. H. Lee, Development of an ASME-NH Program for Nuclear Component Design at Elevated Temperatures, *International Journal of pressure Vessels and Piping*, 85 (2008) 385-393.
[7] G. H. Koo and J. H. Lee, Computer Program of SIE ASME-NH Code, KAERI/TR-3526/2008, KAERI, (2008).
[8] ANSYS User's Manual, Volume I and II.

Gyeong-Hoi Koo received a Ph.D in Mechanical Engineering from KAIST in 1996. He is a principal researcher in KAERI (Korea Atomic Energy Research Institute) since 1989. His expertise in fields of structural engineering are structural vibration, seismic analysis, creep-fatigue design by analysis, buckling analysis, and fatigue monitoring system. Recently he is endorsed as a committee member of ASME Codes and Standards for elevated temperature design for Gen-IV reactors.